Supporting Information for

Understanding the Reaction Mechanism and Performances of 3d Transition Metal Cathodes for All-solid-state Fluoride Ion Batteries

Datong Zhang[1], Kentaro Yamamoto[1], Aika Ochi[1], Yanchang Wang[1], Takahiro Yoshinari[1], Koji Nakanishi[1], Hiroyuki Nakano[1], Hidenori Miki[1,2], Shinji Nakanishi[2], Hideki Iba[2], Tomoki Uchiyama[1], Toshiki Watanabe[1], Koji Amezawa[3], and Yoshiharu Uchimoto[1]*

[1]Graduate School of Human and Environmental Studies, Kyoto University, Yoshida-nihonmatsucho, Sakyo, Kyoto 606-8501, Japan

[2]Battery Research Div., Toyota Motor Corporation, 1200 Mishuku, Shizuoka 410-1193, Japan

[3]IMRAM, Tohoku University, 2-1-1 Katahira, Aoba, Sendai, Miyagi 980-8577, Japan

*Corresponding Author (yamamoto.kentaro.4e@kyoto-u.ac.jp)

ORCID: Kentaro Yamamoto (0000-0002-8739-4246)

Table S1. The parameters of RF sputtering on LaF_3 substrate

Element	Application	Thickness / nm	RF Sputtering Power / W
Cu	Working electrode	2.3	50
Co	Working electrode	2.3	120
Ni	Working electrode	2.3	100
Pb	Reference electrode	1000	50
Pt	Current collector	50	50
W	Current collector	50	120

RF Sputtering Temperature: Room temperature (~25 ˚C)

Atmosphere: Argon

Atmosphere pressure: 1.0 Pa

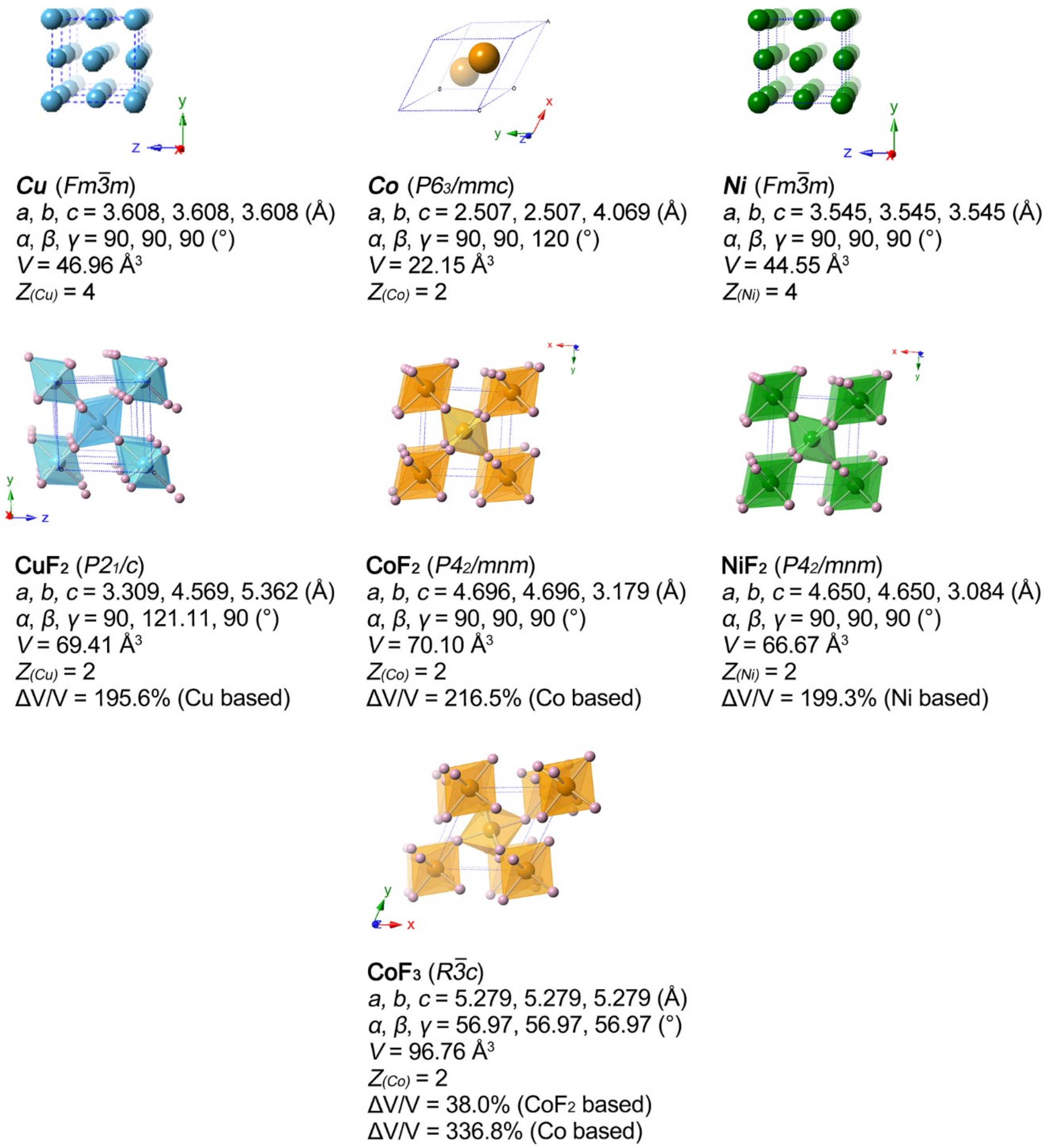

Figure S1. The crystallographic models of Cu, Co, Ni and their fluorides. The volumetric changes are listed under each model. [1-6]

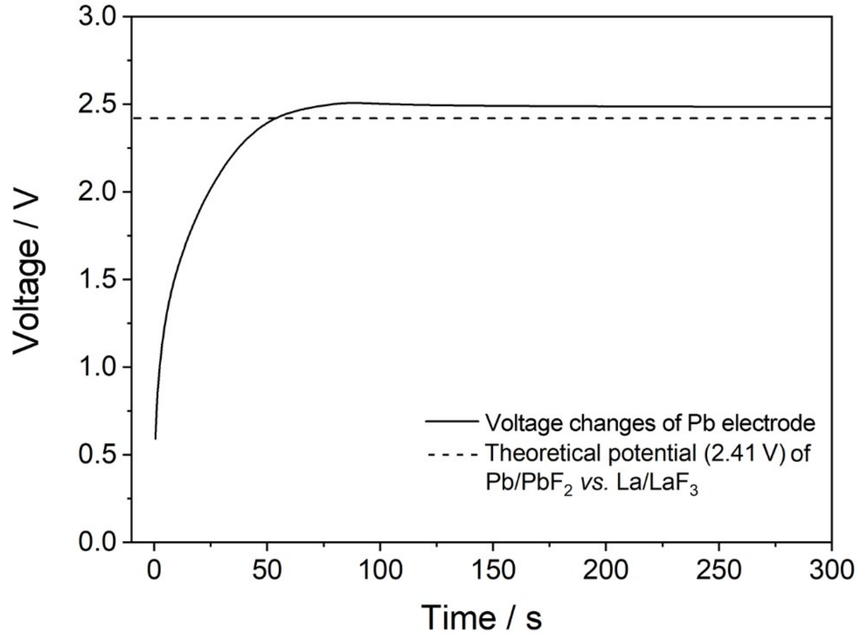

Figure S2. The voltage changes of Pb reference electrode versus counter electrode upon pre-fluorination treatment. The dash line represents the theoretical voltage (2.41 V) of Pb/PbF_2 *vs*. La/LaF_3.

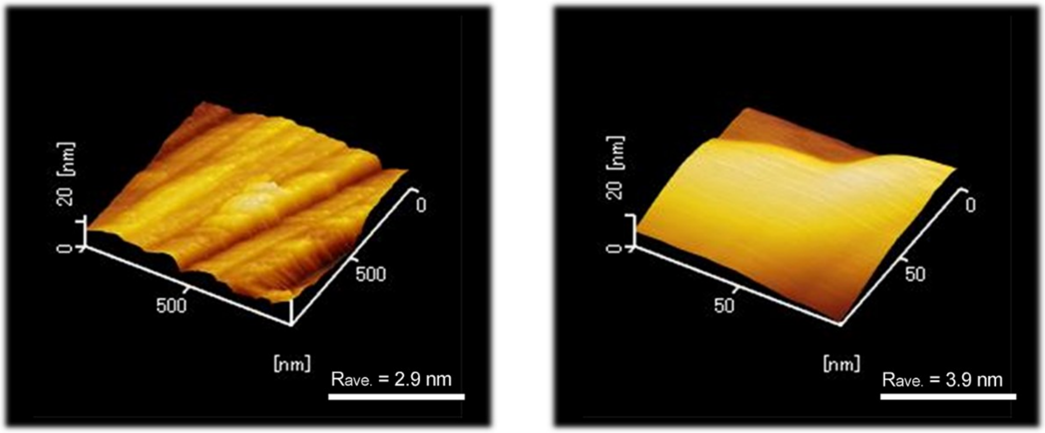

Figure S3. Surface smoothness of the substrate. Atomic force microscopy (AFM) images of (a) mirror polished LaF_3 substrate and (b) Cu deposited LaF_3 substrate. The surface roughnesses of the substrate before and after the Cu deposition are 2.9 and 3.9 nm, respectively.

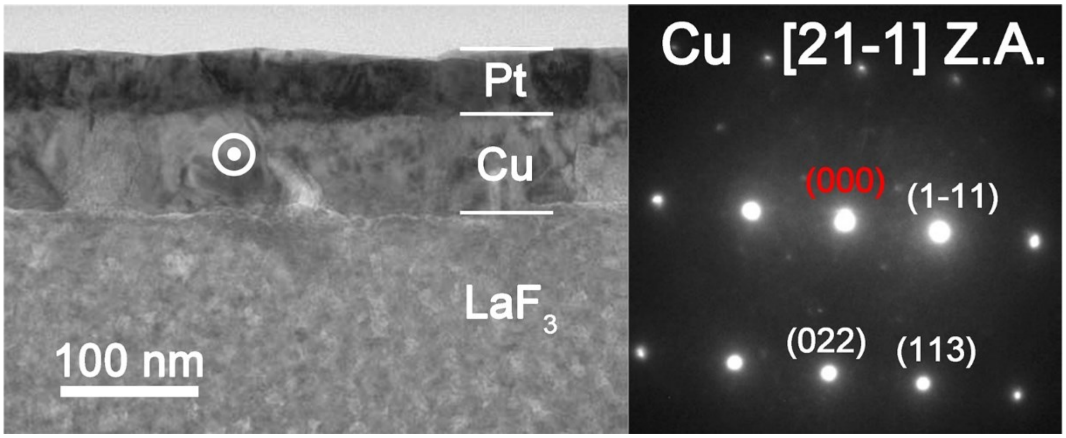

Figure S4. The cross-sectional TEM images of Pt, Cu film and LaF_3 substrates, and the nano-area electron diffraction (NAED) patterns of Cu along $[21\bar{1}]$ zone axis.

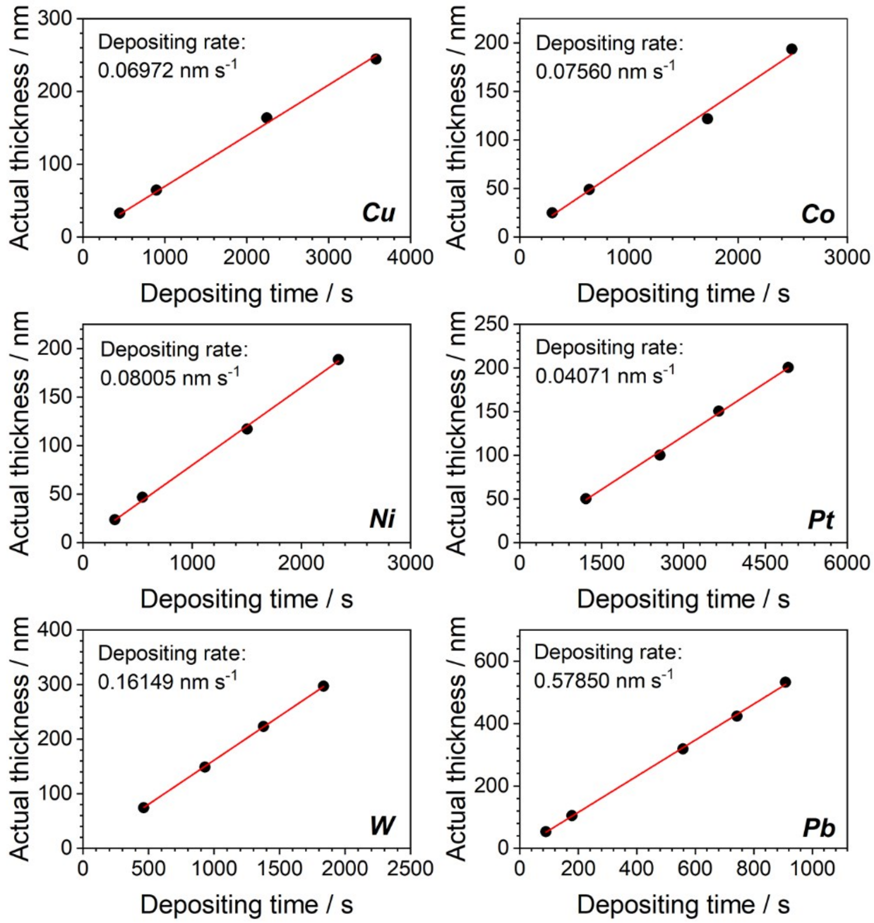

Figure S5. The direct proportional fittings (*y*=*kx* model) of depositing rates of all utilized metals.

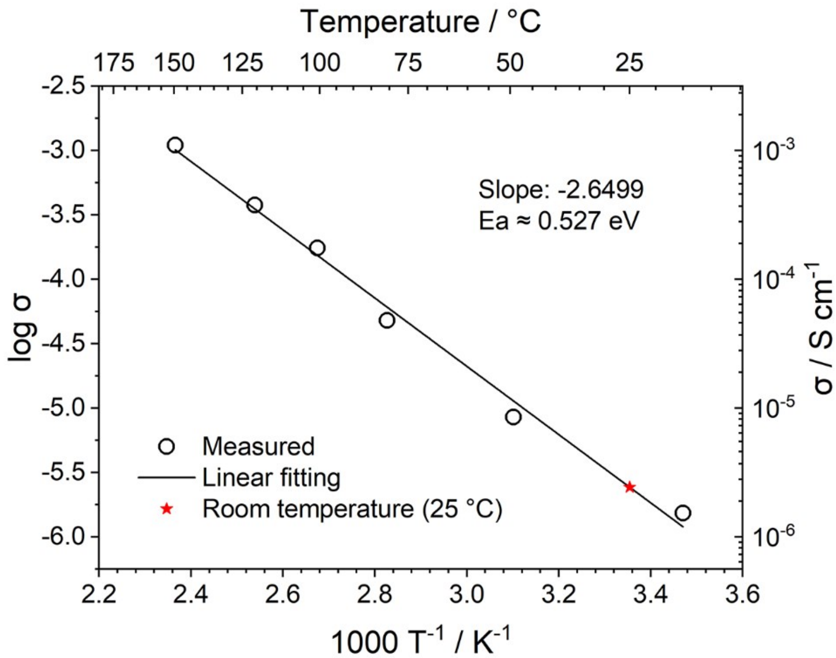

Figure S6. The ionic conductivities of LaF_3 substrates at temperatures of 15, 50, 80, 100, 125, 150 ˚C, respectively, and corresponding Arrhenius linear fitting.

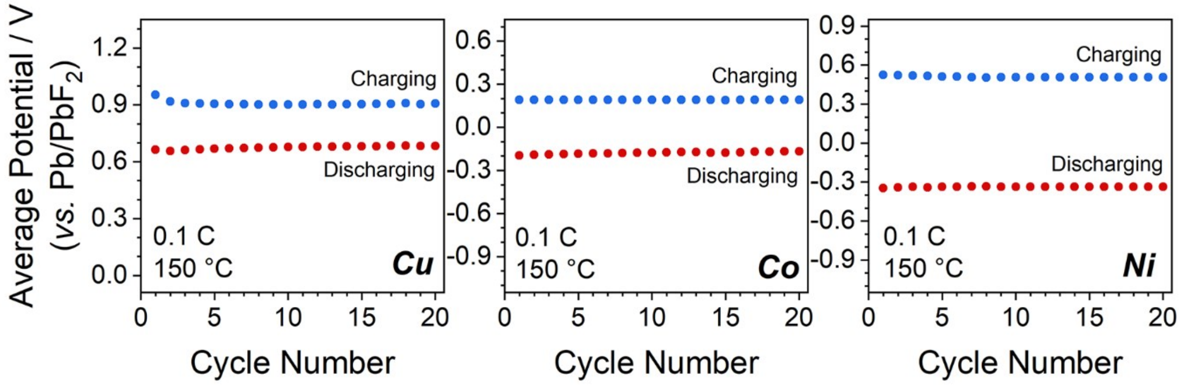

Figure S7. The average working potentials in the first 20 cycles of Cu, Co and Ni at 0.1 C and 150 ˚C.

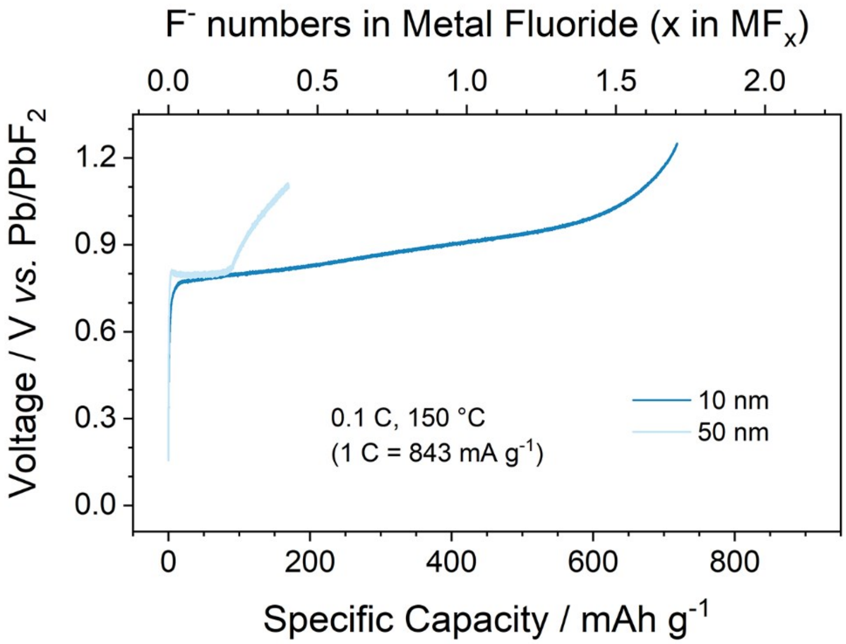

Figure S8. The electrochemical properties of Cu with various thicknesses. The 10 nm sample possessed a similar initial performance with 2.3 nm sample in this study, while the thickest sample only delivered an initial charging capacity of 170 mAh g^{-1} which corresponded to c.a. 20% of theoretical values, i.e. diffusion depth of 10 nm out of 50 nm.

REFERENCES

1. Owen, E. A.; Yates, E. L. Precision measurements of crystal parameters Locality: synthetic Sample: at T = 18 ˚C. *Philos. Mag.* **1933,** *15*, 472-488.

2. Fischer, P.; Hälg, W.; Schwarzenbach, D.; Gamsjäger, H. Magnetic and crystal structure of copper (II) fluoride. *J. Phys. Chem. Solids* **1974,** *35* (12), 1683-1689.

3. Zemann, J. Crystal structures, 2nd edition. Vol. 1 by R. W. G. Wyckoff. *Acta Crystallogr.* **1965,** *18* (1), 139.

4. Jorgensen, J. E.; Smith, R. I. On the compression mechanism of FeF_3. *Acta Crystallogr. Sect. B: Struct. Sci.* **2006,** *62* (Pt 6), 987-992.

5. Costa, M. M. R.; Paixão, J. A.; de Almeida, M. J. M.; Andrade, L. C. R. Charge Densities of Two Rutile Structures: NiF_2 and CoF_2. *Acta Crystallogr. Sect. B: Struct. Sci.* **1993,** *49* (4), 591-599.

6. Hepworth, M. A.; Jack, K. H.; Peacock, R. D.; Westland, G. J. The Crystal Structures of the Trifluorides of Iron, Cobalt, Ruthenium, Rhodium, Palladium and Iridium. *Acta Crystallogr.* **1957,** *10* (1), 63-69.